JOURNAL OF CATALYSIS **163,** 346–353 (1996)
ARTICLE NO. 0336

On the Role of Fe and Co Dopants during the Activation of the $VO(HPO_4)$, $0.5\,H_2O$ Precursor of the Vanadium Phosphorus Catalyst as Studied by *in Situ* Laser Raman Spectroscopy

II. Study of $VO(HPO_4)$, $0.5\,H_2O$ Precursors Prepared by Reduction of $VOPO_4$, $2\,H_2O$ by Isobutanol

M. T. Sananés-Schulz,*,† F. Ben Abdelouahab,‡ G. J. Hutchings,† and J. C. Volta*

*Institut de Recherches sur la Catalyse, CNRS, 2 Avenue A. Einstein, 69626 Villeurbanne Cédex, France; †Leverhulme Centre for Innovative Catalysis, Department of Chemistry, University of Liverpool, P.O. Box 147, Liverpool L69 3BX, United Kingdom; and ‡Faculté des Sciences, Université Abdelmalek Essaadi, BP 2121, Tétouan, Morocco

Received December 18, 1995; revised May 15, 1996; accepted June 3, 1996

Two vanadium phosphorus oxide precursors doped by Co and Fe have been prepared by a new route consisting of a reduction of $VOPO_4$, $2H_2O$ by isobutanol which is known to give a particular morphology of $VOHPO_4$, $0.5H_2O$, developing crystallites in the [110] direction. Their activation under *n*-butane/air catalytic atmosphere (1.5%) has been compared to the corresponding undoped precursor prepared under the same conditions and used as a reference. The modification of the structure of the VPO materials has been followed on-line by *in situ* laser Raman spectroscopy. In a first period of the activation, the nucleation of α_I-$VOPO_4$ is favoured for the undoped VPO precursor, while $(VO)_2P_2O_7$ appears in a second period. For the Co-doped VPO precursor, α_I- and α_{II}-$VOPO_4$ first appear, and then $(VO)_2P_2O_7$ appears. At variance, the Fe-doped VPO precursor promotes the only nucleation of α_I-$VOPO_4$. When comparing with the classical organic route, catalytic performances are markedly improved when the $VOHPO_4$, $0.5H_2O$ precursor is prepared via this new route both for the undoped and the Co-doped VPO catalysts. At variance, the Fe-doped catalyst gives poorer performances which have been explained by a high oxidation state for this catalyst (almost (V^{5+}) as α_I-$VOPO_4$). This is confirmed by an analysis of the bulk and surface composition of the final catalysts by XRD and XPS spectroscopy. The role of the two dopants on this new morphology of $VOHPO_4$, $0.5H_2O$ is then quite different at variance with what was observed on the same precursor prepared by the classical route of reduction of V_2O_5 by isobutanol (see B. Abdelouahab *et al*., 1995, *J. Catal*., 157, 687. The present study demonstrates that the preparative route for the formation of doped VPO precursors is most important in controlling the $VOPO_4/(VO)_2P_2O_7$ dispersion and catalytic performance of the final catalyst.

INTRODUCTION

In previous publications (1–3), we have demonstrated the efficacy of Raman spectroscopy in the study of the physicochemical characteristics of the vanadium phosphorus oxide (VPO) catalysts, in particular during the activation of the vanadyl phosphorus hemihydrate $VOHPO_4$, $0.5H_2O$, which is well known to be the precursor of the VPO catalysts (4). During this activation process, the precursor follows two parallel transformations: first, the topotactic dehydration to vanadyl pyrophosphate $(VO)_2P_2O_7$ and the oxydehydration to $VOPO_4$ phases (γ- and δ-$VOPO_4$, the second one being progressively changed to α_{II}-$VOPO_4$), second, a reduction of the $VOPO_4$ phases to $(VO)_2P_2O_7$ and the crystallinity progressively improves. These changes were recently demonstrated by using techniques which analyzed simultaneously the surface and bulk properties of the VPO material during the first hours of the activation of the precursor (5). The contribution of Raman spectroscopy, particularly in *in situ* conditions, was crucial due to the fact that, for the first time, it evidenced the determining role of V^{5+} species in the $VOPO_4$ structure for the activation of *n*-butane to maleic anhydride (MA) (2). Furthermore, it has been observed by using a TAP-2 reactor system, which permits a combination of steady-flow and high speed transient response, that "equilibrated VPO catalysts" when exposed to an oxygen atmosphere become more reactive and selective to MA formation (6). From such information, it appears that the V^{5+}/V^{4+} local dispersion is controling the reactivity of the VPO catalysts for *n*-butane oxidation to maleic anhydride and that the microstructure of the $VOPO_4/(VO)_2P_2O_7$ interface is of key importance in the course of the activation of the precursor.

In a previous publication we showed that the $VOPO_4/(VO)_2P_2O_7$ dispersion can be modified by using dopants (3). For example Co and Fe dopants have been introduced as acetylacetonate salts in solution in isobutanol during the synthesis of the $VOHPO_4$, $0.5H_2O$ precursor using the organic route which consists in a reduction of V_2O_5 by isobutanol (4). The activation of the doped VPO precursors under *n*-butane/air atmosphere, when studied

0021-9517/96 $18.00

with *in situ* Raman spectroscopy, confirmed the fact, as previously observed (1), that maleic anhydride was produced as soon as $VOPO_4$ structures were simultaneously observed with $(VO)_2P_2O_7$. Doping the bulk of the $VOHPO_4$, $0.5H_2O$ precursor using this procedure (7) favoured the nucleation of the $VOPO_4$ structure at lower temperature and resulted in higher selectivity to MA (3).

It is possible to change the morphology of the $VOHPO_4$, $0.5H_2O$ precursor during its synthesis from V_2O_5 not only by changing the reducing alcohol (8) but also by using a new route which consists of a reduction of $VOPO_4$, $2H_2O$ by isobutanol (9). This new approach gives a specific morphology of the vanadyl phosphohemihydrate with a marked growth of the crystallites in the [110] direction together with limited development in the [001] direction. This corresponds to thin platelets developing the (001) crystal faces.

In this publication we use *in situ* Raman spectroscopy to study the activation of the $VOHPO_4$, $0.5H_2O$ precursor prepared by reduction of $VOPO_4$, $2H_2O$ by isobutanol and to compare with the same precursor material when doped by iron and cobalt ($M/V = 5\%$). Results are compared with those of a previous study (3).

EXPERIMENTAL

Preparation of the Undoped and Co- and Fe-Doped VPO Precursors

Undoped and doped VPO precursors were prepared via $VOPO_4$, $2H_2O$ (9). $VOPO_4$, $2H_2O$ was prepared from V_2O_5 (12.0 g) and H_3PO_4 (115.5 g, 85%) which were refluxed in water (24 ml H_2O/g solid) for 8 h. The resulting $VOPO_4$, $2H_2O$ was recovered by filtration and washed with water and finally identified by XRD. Then 4 g of this solid was refluxed with isobutanol (80 ml) for 21 h, and the resulting solid was recovered by filtration and dried in air (110°C, 16 h) (9). It will be denoted VPD.

For the preparation of the two doped precursors (M = Fe, Co; atomic ratio, V : M = 1 : 0.05), the required mass of the corresponding acetylacetonate salts were previously dissolved in isobutanol according to the atomic M/V stoichiometry, prior to refluxing $VOPO_4$, $2H_2O$ with isobutanol. The same procedure was followed as for the undoped precursor. These are denoted CoVPD and FeVPD.

The three precursors were then dried at 120°C in air for 12 h.

Precursors and Catalyst Characterization

A schematic diagram of the *in situ* cell and the associated GC analysis using a FID detector has been described previously (1–3). The system permits simultaneous collection of the Raman spectra with the catalytic results in the course of the reaction. The spectrophotometer (DILOR OMARS 89) was equipped with an intensified photodiode array detector. The emission line at 514.5 nm from an Ar^+ ion laser (SPECTRA PHYSICS, Model 164) was used for excitation. The power of incident beam on the sample was 30 mW. Time of acquisition was adjusted according to the intensity of the Raman scattering. One hundred spectra were accumulated for each spectrum in order to improve signal to noise ratio. The wavenumber values obtained from the spectra were accurate to within about 2 cm^{-1}. To reduce both thermal and photodegradation of samples, the laser beam was scanned on the sample surface by means of a rotating lens. The scattered light was collected in the back scattering geometry.

The three precursors and the VPO catalysts after examination by *in situ* laser Raman spectroscopy were characterised by XRD diffraction using a Siemens diffractometer using Cu $K\alpha$ radiation. XPS examinations of the VPO materials were performed with an ESCALAB 200 R machine using the Al $K\alpha$ radiation. The binding energy of adventitious carbon was taken as reference at 284.5 eV. Examination was directed towards binding energies of P_{2p}, C_{1s}, $V_{2p}^{3/2}$ (V^{5+} and V^{4+}), $Co_{2p}^{3/2}$, $Fe_{2p}^{3/2}$, and O_{1s}. The catalysts were briefly exposed to air in the course of their deposit on the sample holder. In preliminary experiments, we observed that air exposure at room temperature, at least for a few minutes, did not induce significant changes in the XPS results.

RESULTS

Analysis of the Undoped and Doped Precursors

Chemical analysis showed that Co and Fe are present in the two $VOHPO_4$, $0.5H_2O$ structures with the expected Co/V atomic ratios (5%). A STEM examination of the two doped precursors showed a good dispersion into the structure of the grains for the Co and Fe promotors (10).

Doping by Co does not modify significantly the surface area of the undoped precursor (30.9 m^2/g for VPD and 26.5 m^2/g for CoVPD), while doping with Fe does (7.5 m^2/g).

Figure 1 shows the XRD spectra of the doped precursors as referred to the undoped one. The characteristic lines of $VOHPO_4$, $0.5H_2O$ are observed for VPD (3) with a small contribution of α_I-$VOPO_4$ with the characteristic (001) line at 21° 2Θ. An intense (220) line is observed for $VOHPO_4$, $0.5H_2O$ as referred to the (001) of the ASTM file. Doping with Co does not modify the XRD pattern, whereas the XRD pattern is quite different for FeVPD which is characteristic of the α_I-$VOPO_4$ phase alone (3). In this case, the $VOHPO_4$, $0.5H_2O$ phase is totally absent.

Study of the Activation of the Undoped and Doped $VOHPO_4$, $0.5H_2O$ as Studied by in situ Raman Spectroscopy

It is unfortunate that no information can be obtained from the Raman spectra of VPD, CoVPD, and FeVPD

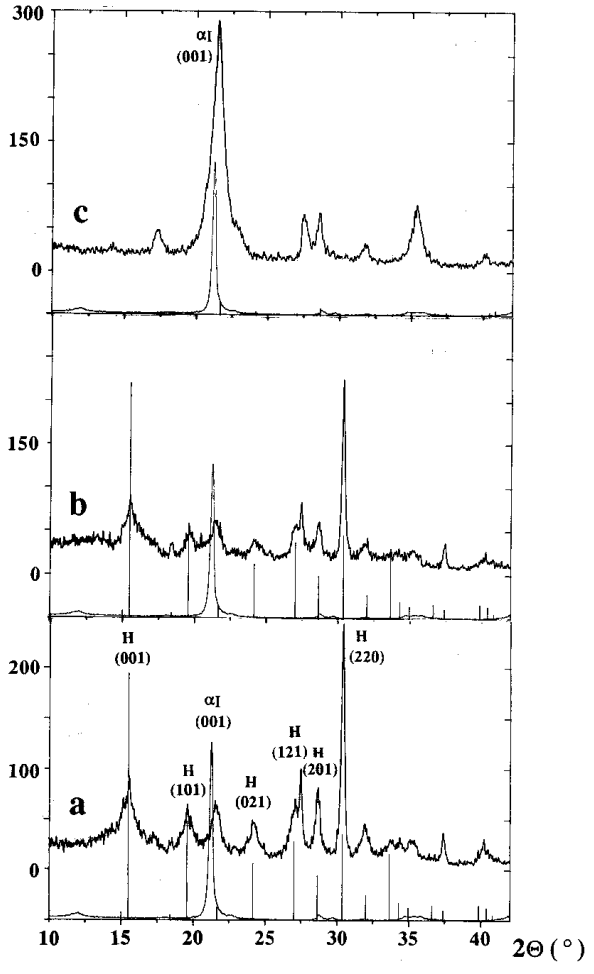

FIG. 1. XRD spectra of the three precursors. (a) VPD, (b) CoVPD, (c) FeVPD, spectra are referenced to the vanadyl phosphate hemihydrate (H) and to α_I-$VOPO_4$ (α_I).

from room temperature up to 230°C, due to a high level of fluorescence of the materials. This has been previously explained by the presence of isobutanol molecules trapped into the layer structure of the precursor (3).

Figures 2 and 3 show the evolution of the Raman spectra of the undoped VPD precursor when temperature is increased under the *n*-butane/air mixture from 234°C (temperature of the first detection of MA) up to 430°C ($\Delta T = 1.25$°C min^{-1}) (Fig. 2) and then maintained at 430°C for a long period (Fig. 3). The band at 1030–1040 cm^{-1} is characteristic of α_I-$VOPO_4$ phase, while the band at 930 cm^{-1} is not specific to any particular VPO phase since it can be indexed to all VPO phases ($VOPO_4$ and $(VO)_2P_2O_7$) (3). No significant changes are observed with increasing temperature except that the intensity of the two bands decreases. Spectra at 430°C (Fig. 3) show a more defined band at 1176 cm^{-1} and a contribution in the 1120 cm^{-1} range which are both characteristic of $(VO)_2P_2O_7$. This is indicative of the progressive crystallization of this phase with time. The

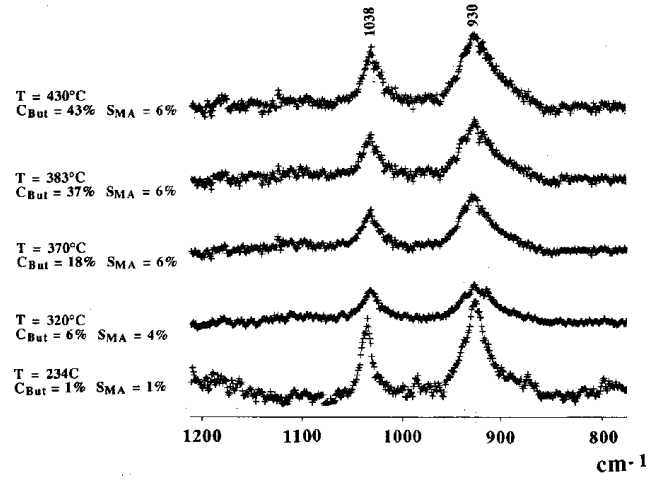

FIG. 2. Raman spectra obtained by treatment of the VPD precursor from 234 up to 430°C under catalytic mixture ($\Delta T = 1.25$°C min^{-1}).

band at 1038 cm^{-1}, characteristic of α_I-$VOPO_4$, is still very intense.

The catalytic results, which are given in Fig. 2, confirm the observation of MA as soon as the $VOPO_4$ structure is observed by Raman spectroscopy. By comparison with the *in situ* activation of the $VOHPO_4, 0.5H_2O$ precursor prepared according to the organic route (VPO) (3), it appears that best performance is obtained at lower temperature for VPD due to the nucleation of $VOPO_4$ structures (V^{5+} sites) at a lower temperature. This is particularly apparent for Fig. 3

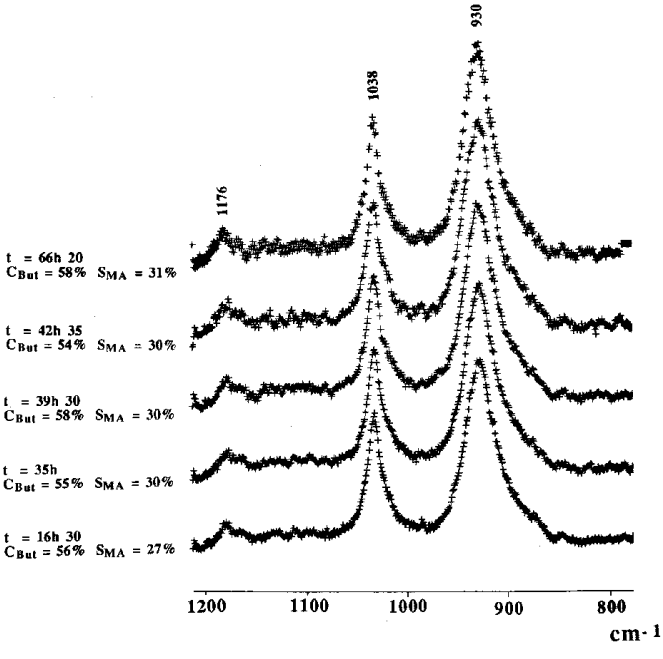

FIG. 3. Raman spectra at 430°C of the VPD catalyst obtained by treatment of the VPD precursor under catalytic mixture.

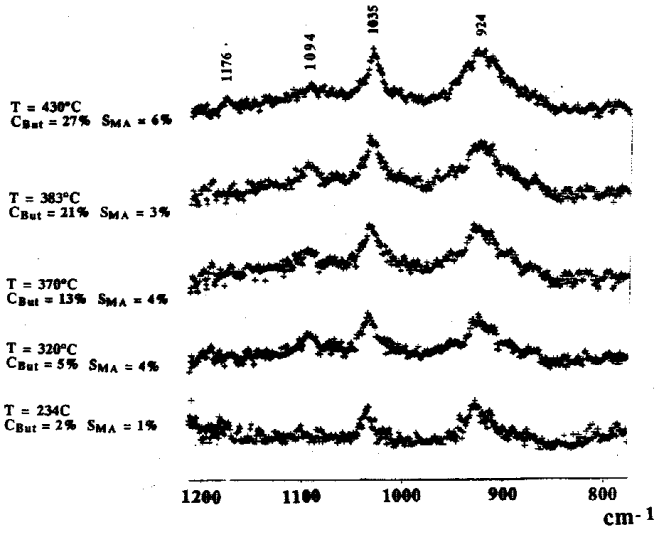

FIG. 4. Raman spectra obtained by treatment of the CoVPD precursor from 234 up to 430°C under catalytic mixture ($\Delta T = 1.25$°C min^{-1}).

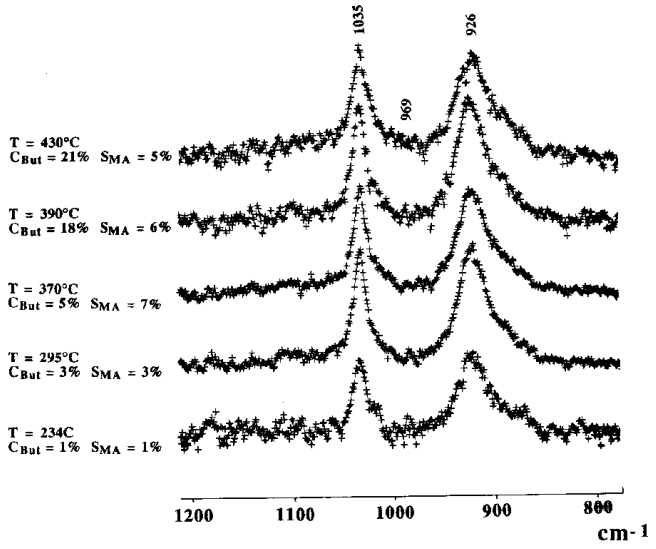

FIG. 6. Raman spectra obtained by treatment of the FeVPD precursor from 234 up to 430°C under catalytic mixture ($\Delta T = 1.25$°C min^{-1}).

when considering MA selectivity as the catalyst crystalizes at 430°C (see Fig. 5 in Refs. (3)).

Figures 4 and 5 show the evolution of the Raman spectra of the CoVPD precursor when temperature is increased under the *n*-butane/air mixture from 234°C (temperature of the first detection of MA) up to 430°C ($\Delta T = 1.25$°C min^{-1}) (Fig. 4) and then maintained at 430°C for a long period (Fig. 5). In addition to the two bands observed at 1035 and 924 cm^{-1} and at variance with the undoped VPD (Fig. 2), a new band appears at 1094 cm^{-1} from 320 to 430°C. This band is characteristic of the α_{II}-$VOPO_4$ structure (3).

No significant difference is detected in the catalytic results which indicates that α_I- and α_{II}-$VOPO_4$ play a similar catalytic role on the disorganized VPO matrix.

Figure 5 shows a comparable evolution with time at 430°C both of the Raman spectra and of the catalytic results as compared with the VPD catalyst (Fig. 3).

Figures 6 and 7 show the evolution of the Raman spectra of the FeVPD precursor when temperature is increased under the *n*-butane/air mixture from 234°C (temperature

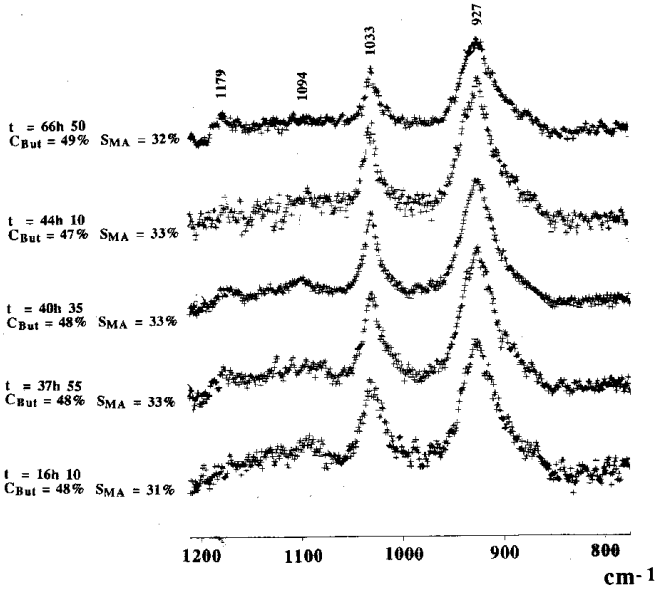

FIG. 5. Raman spectra at 430°C of the CoVPD catalyst obtained by treatment of the CoVPD precursor under catalytic mixture.

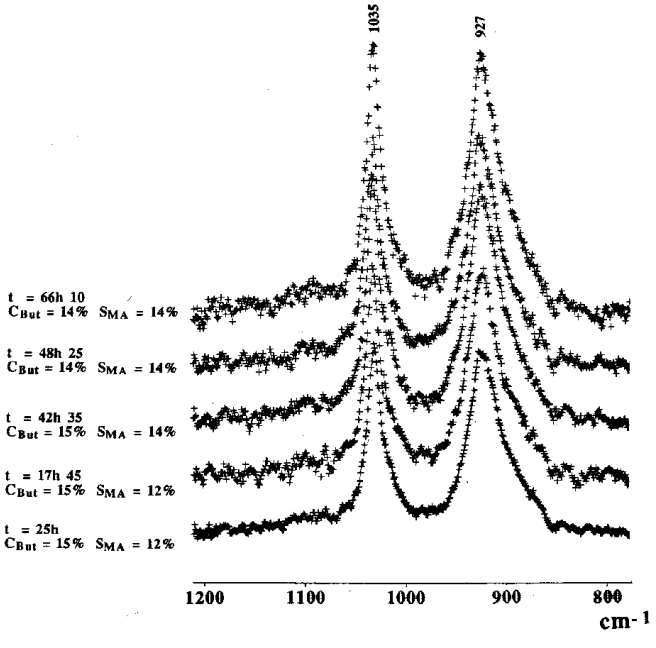

FIG. 7. Raman spectra at 430°C of the FeVPD catalyst obtained by treatment of the FeVPD precursor under catalytic mixture.

of the first detection of MA) up to 430°C ($\Delta T = 1.25$°C min^{-1}) (Fig. 6) and then maintained at 430°C for a long period (Fig. 7). The spectra in Fig. 6 are similar to spectra of Fig. 3 but the intensity of the band at 1035 cm^{-1} characteristic of α_I-$VOPO_4$ is much higher than that of the band at 926 cm^{-1}, which gives to all spectra features of the pure α_I-$VOPO_4$ phase as published in Ref. (3). This structure is confirmed for the spectra of Fig. 7 which appear all characteristic of the α_I-$VOPO_4$ phase. No bands at 1176 and 1125 cm^{-1} characteristic of any $(VO)_2P_2O_7$ are observed on high temperature spectra on Fig. 7.

In this case, catalytic results are significantly poorer in terms of both activity and selectivity than the VPD and CoVPD catalysts at the same temperature.

Characterisation of Undoped and Doped VPD Catalysts after in situ Raman Examination

Figure 8 shows the XRD spectra of the catalysts after the *in situ* Raman examination. VPD is characteristic of a mixture of the two $(VO)_2P_2O_7$ and α_I-$VOPO_4$ phases, which is also the case for the CoVPD catalyst. XRD spectra for these two catalysts are very similar. Note that the relative intensities of the $(VO)_2P_2O_7$ reflections are the same for VPD and CoVPD and this shows that the corresponding crystallites present the same morphology after doping with Co. FeVPD shows only the α_I-$VOPO_4$ phase and the $(VO)_2P_2O_7$ structure is absent. The characterisation by XRD confirms the Raman examination of the three catalysts.

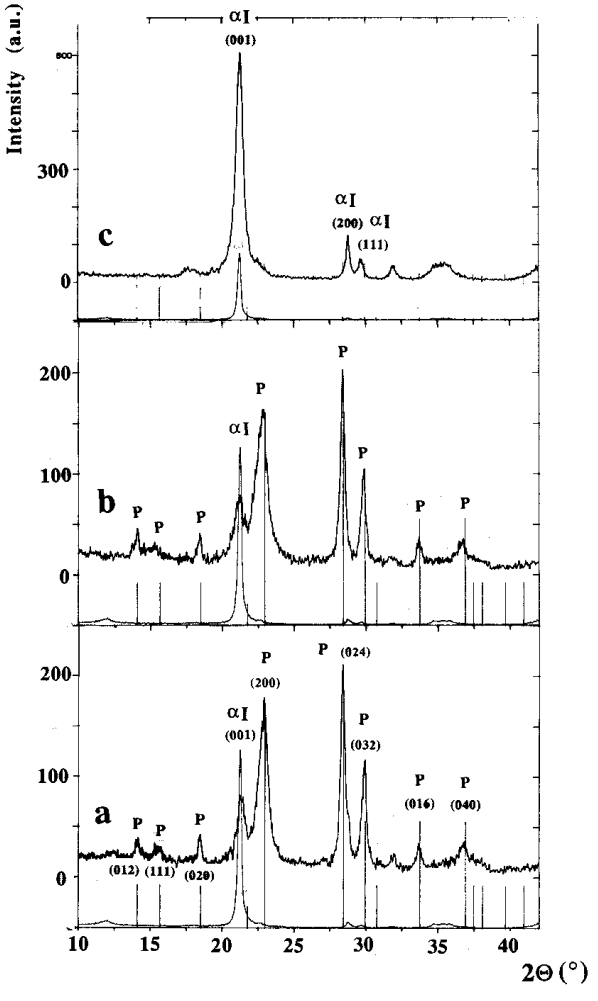

FIG. 8. XRD spectra of the three catalysts after *in situ* Raman examination. (a) Activated VPD, (b) activated CoVPD, (c) activated FeVPD.

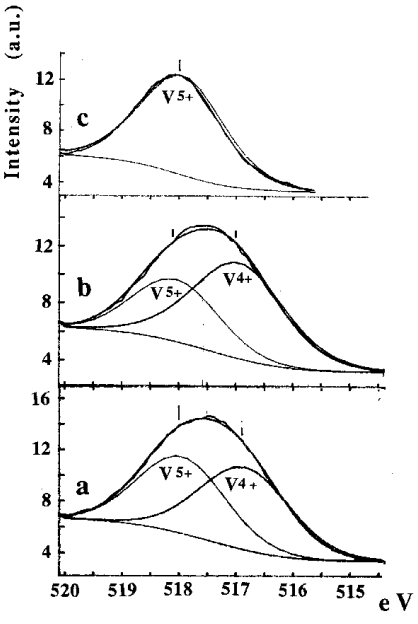

FIG. 9. XPS spectra showing the V2p 3/2 signal of the three catalysts after *in situ* Raman examination. (a) Activated VPD, (b) activated CoVPD, (c) activated FeVPD. (referred to Cls: 284.5 eV).

XPS measurements have been performed on the three catalysts. Previous studies have shown that binding energies for V2p3/2 level for V^{4+} and V^{5+} are observed at 516.9 eV and 518.0 eV, respectively, and separated by 1 eV (11, 12, 5) (Fig. 9). Due to the contribution of these two oxidation states of vanadium, the V2p3/2 peak is relatively broad (2.3–

TABLE 1

XPS Results on the Three Catalysts after *in Situ* Raman Examination

Catalysts	Undoped VPD	CoVPD	FeVPD
BE P_{2p} (eV)	131.7	131.7	131.7
BE $V^{5+}2p$ (eV)	518.0	518.0	517.8
BE $V^{4+}2p$ (eV)	516.9	516.9	516.7
BE O_{1s} (eV)	730.5	730.5	730.5
P/V (%)	1.80	1.87	2.10
V^{5+}/V (%)	47.0	37.0	100
V^{4+}/V (%)	53.0	63.0	0
V^{5+}/V^{4+} (%)	89.0	59.0	∞

Note. BE, binding energies.

2.4 eV). The percentage of surface V^{4+} and V^{5+} of the three catalysts (as determined by XPS) has been calculated using a deconvolution method (5). Results are shown in Table 1. We observe a slight P enrichment when doping with Co and a much higher one when doping with Fe. Doping with Co results in a decrease of the V^{5+} contribution (from 47 to 37%), while the surface of V^{5+} appears totally oxidised as V^{5+} when doping with Fe, in agreement with the detection of only the α_I-$VOPO_4$ (V^{5+}) phase by Raman and XRD. It is noticeable that an air exposure at room temperature does not affect the XPS spectra of the VPO catalysts and thus does not affect the oxidation state of surface vanadium species.

DISCUSSION OF RESULTS—A COMPARISON OF THE EFFECTS OF THE Co AND Fe DOPANTS DEPENDING ON THE MODE OF PREPARATION OF THE PRECURSOR

We have previously shown that a particular morphology of the $VOHPO_4$, $0.5H_2O$ precursor is obtained using the new route for the reduction of $VOPO_4$, $2H_2O$ by isobutanol (9). The precursor has crystallites with mainly (001) basal planes. This has been confirmed by the examination of the undoped reference precursor VPD by XRD and SEM. The present study shows a very different effect of the two dopants, Co and Fe, on the precursor when they are introduced via acetylacetonate salts dissolved in isobutanol. While Co hardly changes the structure of the VPD precursor, Fe oxidizes it almost completely to α_I-$VOPO_4$.

The characterisation and the differentiation of the VPD, CoVPD, and FeVPD by Raman is impossible at room temperature due to fluorescence generated by the isobutanol molecules trapped in the layer structure of the materials. *In situ* Raman examination under the *n*-butane/air reaction atmosphere permits spectra to be obtained as soon as the temperature reaches 230°C. At this temperature, the fluorescence has almost disappeared and the spectra show the formation of the α_I-$VOPO_4$ structure for the three activated precursors. In addition, CoVPD shows the α_{II}-$VOPO_4$, structure. At this low temperature, maleic anhydride (MA) is detected. The simultaneous presence of the $(VO)_2P_2O_7$ structure (small signal at 1176 cm^{-1}) is difficult to ascertain on the activated VPD and Co VPD, but is observed at the higher temperature of activation. In the case of the activated FeVPD, $(VO)_2P_2O_7$ is almost absent whatever the temperature considered. The comparison of the Raman spectra at 430°C associated with the catalytic results from the three activated catalysts shows the necessity to associate the $VOPO_4$ structures (α_I- and α_{II}-$VOPO_4$ in this study) with the $(VO)_2P_2O_7$ structure to reach the best catalytic performance. It also demonstrates that the absence of $(VO)_2P_2O_7$, in the case of the activated FeVPD, is detrimental.

Differences are observed on the effect of the Co and Fe dopants depending on the morphology of this precursor induced by different preparative routes. In this discussion, we compare results obtained from $VOHPO_4$, $0.5H_2O$ precursors doped according to the organic route of reduction of V_2O_5 by isobutanol (see Ref. 1) (these precursors are coded VPO, CoVPO, and FeVPO) with results obtained from doping the $VOHPO_4$, $0.5H_2O$ precursor according to the new route of reduction of the $VOPO_4$, $2\,H_2O$ dihydrate by isobutanol (precursors are coded VPD, CoVPD, and FeVPD, this study). In both cases, the doping elements are dissolved in the isobutanol, the reducing agent, to favour the best situation for dispersing the dopants.

While Co hardly affects the morphology of the $VOHPO_4$, $0.5H_2O$ precursor on VPO and VPD, Fe affects the morphology in the case of VPO and changes the structure to α_I-$VOPO_4$ for VPD.

A common feature observed for the VPO and VPD series is that the nucleation of the $VOPO_4$ structures is associated with the formation of MA. The VPO series favours first the δ-, γ-, and α_{II}-$VOPO_4$ structures, while the VPD series favours first the α_I- and α_{II}-$VOPO_4$ structures. There does not appear to be a specific catalytic role of one of these two structures. The simultaneous presence of $(VO)_2P_2O_7$ at the moment of the first detection of MA is questionable due to difficulty in ascertaining presence by Raman (the only univocal signal characteristic of this phase is poorly intense at 1176 cm^{-1}). Nevertheless, a previous study on the VPA precursor prepared according to the aqueous route, for which fluorescence is almost absent, shows the simultaneous presence of the $VOPO_4$ (V^{5+}) and $(VO)_2P_2O_7$ (V^{4+}) structures when MA is detected. It is also obvious that the nucleation of the $VOPO_4$ structures associated with MA is favoured at lower temperature on the two VPO and VPD series whether doping by Co or Fe. This can be explained by a favourable effect of the redox of the dopants on the V^{5+}/V^{4+} couple.

The XPS study provides interesting information for the P/V surface ratio and on the surface V^{5+}/V^{4+} distribution on the catalysts after the *in situ* activation (compare Table 1 in Ref. (1) with Table 1 in this article). For both the VPO and the VPD series, doping enriches the surface in phosphorus, while, for the VPO series, doping by Co increases the V^{5+}/V^{4+} ratio (from 0.21 to 0.30), and doping by Fe decreases this ratio (0.14). This effect is quite different in the case of the VPD series: doping by Co decreases the V^{5+}/V^{4+} ratio (from 0.89 to 0.59), while doping by Fe changes totally V^{4+} to V^{5+}.

In Fig. 10 we have gathered the Raman spectra for the two VPO and VPD series, registered at 380°C, under the reactive *n*-butane/air atmosphere, at the end of the activation period of the precursors (78 h time-on-stream), simultaneously with the catalytic performance data. The V^{5+}/V^{4+} ratio has been evaluated from the relative ratio

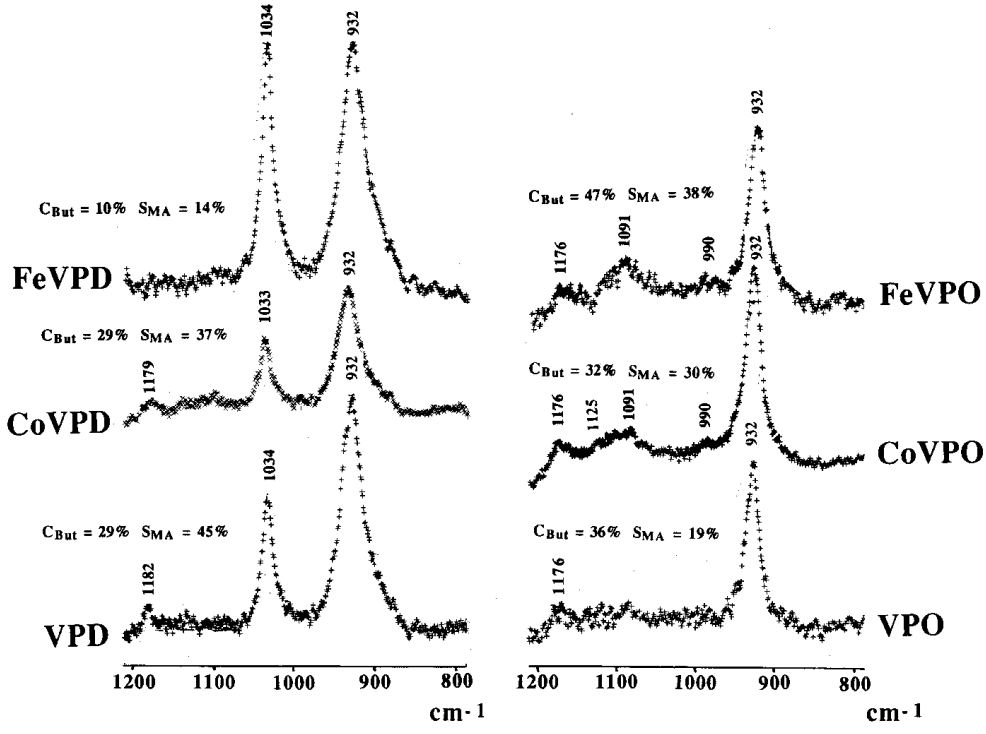

FIG. 10. Comparison of the Raman spectra and the catalytic performances of VPD, CoVPD, FeVPD, VPO, CoVPO, and FeVPO registered at 380°C.

of the intensity of the characteristic bands associated to $VOPO_4$ and $(VO)_2P_2O_7$ structures (1034 cm^{-1} for α_I-$VOPO_4$, 1091 cm^{-1} for α_{II}-$VOPO_4$, and 1176 cm^{-1} for $(VO)_2P_2O_7$, respectively). The selectivity to MA, S_{MA}, has been plotted (Fig. 11a) versus the V^{5+}/V^{4+} ratio (as measured by Raman) for the four catalysts VPO, CoVPO, VPD, and CoVPD, which present comparable level on *n*-butane conversion (around 30%). A monotonic correlation is observed between S_{MA} and this ratio. The same type of correlation, with the same order for the catalysts, is observed when plotting S_{MA} versus the V^{5+}/V^{4+} ratio (Fig. 11b) (as determined by XPS). The MA formation appears thus to be directly correlated with the surface V^{5+}/V^{4+} ratio. From the position of the VPO and VPD points in Fig. 11, it is apparent that doping by Co has a beneficial effect on the VPO series but a detrimental one on the VPD one. No conclusion has been drawn for FeVPO and FeVPD which present quite a different level of conversion and different catalyst structures.

CONCLUSIONS

Raman spectroscopy is a powerful technique with which to follow the *in situ* activation of the $VOHPO_4$, $0.5H_2O$ precursor, particularly in detecting the formation of $VOPO_4$ structures. We have shown that different morphologies of the precursor can influence the kinetics of the two parallel routes (oxydehydration and dehydration) which control, respectively, the nucleation of the $VOPO_4$ structures and the nucleation of the $(VO)_2P_2O_7$ phase and their relative dispersion.

$VOPO_4$, $0.5H_2O$ precursor prepared by the dehydration and reduction of $VOPO_4$, $2H_2O$ with isobutanol favours, during the activation, the nucleation of the $VOPO_4$ species (α_1-$VOPO_4$) on the (100) face of $(VO)_2P_2O_7$ at low temperature and this gives rise to the best catalyst.

The effect of doping depends not only on the nature of the dopant, but also on the morphology of the precursor. Doping permits the control of the local $VOPO_4/(VO)_2P_2O_7$ dispersion during the activation process and this factor should also be highly important for industrial catalysts and should be monitored for "equilibrated catalysts" after long time-on-stream.

A comparison of the catalytic performance (selectivity to MA at isoconversion of *n*-butane) for four VPO catalysts differing by their morphology and the presence or the absence of dopant with characterisation information derived from Raman and XPS has enabled us to conclude that the activation of *n*-butane to MA occurs on $VOPO_4$ domains (V^{5+}) situated in the (100) basal face of $(VO)_2P_2O_7$. We postulate that the catalytic performance would depend on this dispersion which can be influenced by promotors and this emphasizes the importance of studying the microstructure in the (100) basal face of $(VO)_2P_2O_7$. More information is presently needed, at this time, on this point. Indeed, it has been observed by high resolution electron microscopy (14)

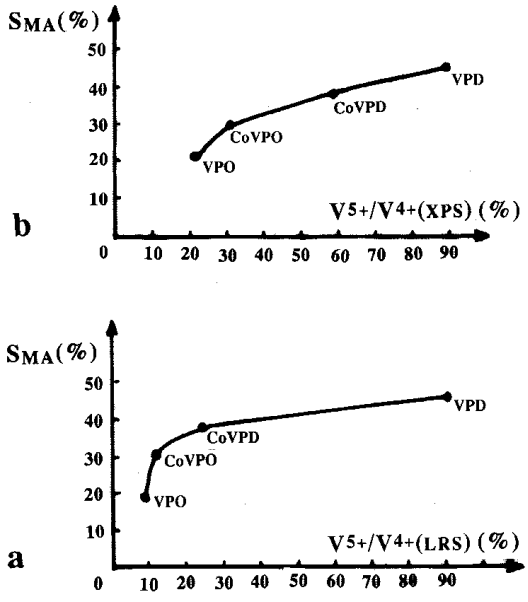

FIG. 11. Selectivity to maleic anhydride (S_{MA}) as versus (a) of V^{5+}/V^{4+} ratio (from the Laser Raman study), (b) of V^{5+}/V^{4+} ratio (from the XPS study).

that increasing the time of the activation of a vanadyl(IV) pyrophosphate catalyst results in a progressive disappearance of an amorphous VPO layer on top of the (100) face of $(VO)_2P_2O_7$. This parallels the ordering of the (100) planes at the surface of $(VO)_2P_2O_7$ with the increase of the selectivity to maleic anhydride (14). The exact nature of the active sites is still debated.

ACKNOWLEDGMENTS

The authors thank the Ecole Centrale de Lyon where the Raman experiments have been performed. We also thank the EC (Contract CHRX-CT92-0065) for financial support.

REFERENCES

1. Ben Abdelouahab, F., Olier, R., Guilhaume, N., Lefebvre, F., and Volta, J. C., *J. Catal.* **134**, 151 (1992).
2. Hutchings, G. J., Desmartin-Chomel, A., Olier, R., and Volta, J. C., *Nature* **368**, 41 (1994).
3. Ben Abdelouahab, F., Olier, R., Ziyad, M., and Volta, J. C., *J. Catal.* **157**, 687 (1995).
4. Johnson, J. W., Johnston, D. C., Jacobson, A. J., and Brody, J. F., *J. Am. Chem. Soc.* **106**, 8123 (1984).
5. Abon, M., Bere, K. E., Tuel, A., and Delichere, P., *J. Catal.* **156**, 28 (1995).
6. Shuurman, Y., and Gleaves, J. T., "Proceedings, 14th North American Meeting of the Catalysis Society, Snowbird, USA, June 11–16, 1995."
7. Ben Abdelouahab, F., Ziyad, M., Leclercq, C., Millet, J. M., Olier, R., and Volta, J. C., *J. Chim. Phys.* **92**, 1320 (1995).
8. Ellison, I. J., Hutchings, G. J., Sananés, M. T., and Volta, J. C., *J. Chem. Soc. Chem. Commun.* 1093 (1994).
9. Hutchings, G. J., Olier, R., Sananés, M. T., and Volta, J. C., *in* "New Developments in Selective Oxidation" (V. Cortés Corberan and S. Vic Bellon, Eds.), Vol. 82, p. 213. Elsevier, Amsterdam, 1994.
10. Kiely, C., Sananés, M. T., Hutchings, G. J., and Volta, J. C., *J. Catal.* in press.
11. Garbassi, F., Bart, J. C., Tassinari, R., Vlaic, G., and Lagarde, P., *J. Catal.* **98**, 317 (1986).
12. Moser, T. P., and Schrader, G. L., *J. Catal.* **104**, 99 (1987).
13. Volta, J. C., Bere, K., Zhang, Y. J., and Olier, R., *in* "ACS Symposium Series, 523" (S. T. Oyama and J. Hightower, Eds.), p. 317. American Chemical Society, Washington, DC, 1993.
14. Guliants, V. V., Benziger, J. B., Sundaresan, S., Yao, N., and Wachs, I. E., *Catal. Lett.* **32**, 379 (1995).